Preparation and thermo-mechanical characterisation of graphene nanoplatelets/low density polyethylene composites

F Pinto[1], G Carotenuto[2], M Meo[1,],*

(1) Material Research Centre, Department of Mechanical Engineering, University of Bath, Bath BA2 7AY, UK

(2) Institute of Composites and Biomedical Materials. National Research Council. Piazzale Tecchio, 80 – 80125 Napoli, Italy.

Abstract

The thermo-mechanical properties of graphene/low density polyethylene (LDPE) composites were investigated and characterised to understand the effect of nanoscaled reinforcement in the thermoplastic matrix. Results show that the presence of the filler does not produce a change in the microscopic structure of the polymer. However, on a macroscopic scale, graphene platelets limit the mobility of the polymer chains, resulting in an increase in stiffness and in some cases, strength of the composite. Orientation of graphene in the LDPE matrix was evaluated by testing composites made with two different manufacturing techniques (compression moulding and blown extrusion). A comparison between experimental data and predictions using the Halpin-Tsai model shows that the orientation of graphene due to the extrusion process leads to better mechanical properties than those obtained with the randomly oriented graphene resulting from the compression moulding technique.

* Corresponding author : Tel: +44 (0)1225 38 4224
E-mail address: m.meo@bath.ac.uk (M. Meo)

1. Introduction

The past thirty years have seen increasingly rapid advances in composites technology, because of the possibility to "tailor" the properties of the material to the needs of different customers.

Recent developments in the field of nanotechnology have led to renewed interest in a particular class of material known as polymer nanocomposites, in which nanoscale filler materials are added to a polymeric matrix in order to enhance mechanical and physical properties. Several studies have proved that when one of the dimensions of the filler is in the range of 10^{-9} m, the resulting polymer based nanocomposite exhibits unique physical, chemical and mechanical properties, compared with composites reinforced with the same quantity of microparticles [1].

The difference between conventional reinforcements and the nanoscale fillers can be explained by the reduction of the nanoparticles' dimensions which increases the surface in contact with the polymeric matrix, generating so-called "nanoeffects" within the composite structure [2-4]. From a structural point of view, a nanocomposite can be defined as a material in which one of its components has at least one nanometric dimension, therefore, we can distinguish three different categories: a) zero dimensional (metal and ceramic nanoparticles), b) mono-dimensional (carbon nanotubes and inorganic nanowires), c) bi-dimensional (nanoclays, graphene). Nanoclays are nanoparticles based mostly on alumina and silica organised in a layered structure in which each layer consists in a sequence of tetrahedric and octahedric nanometric sheets. Because of their dimensions, when embedded within a polymeric matrix, these bi-dimensional nanofiller are able to improve the overall properties of the system, improving mechanical, thermal and chemical properties.

Graphite also shows a similar planar structure, however since natural graphite (NG) is not reinforcing in nature, a high temperature heat treatment is used to modify it to expanded graphite, resulting in a swollen material characterised by low density and high temperature resistance. The low cohesion of this high-porous structure allows it to be partially disaggregated by the application of an intensive sonication treatment, leading to the formation of graphite nanoplatelets, which are characterised by excellent mechanical and physical properties.

The thickness of graphite nanoplatelets can vary from several to dozens of nanometres while the other two dimensions are in the micron scale, resulting in a unique aspect ratio and high specific surface area (2630-2965 m^2/g for completely exfoliated graphene sheets [5]).

Compared with nanoclays, graphite nanoplatelets exhibit lower mass density and due to the sp_2-hybridized carbon atoms bonds plus the absence of electron scattering phenomena, they show a high electrical and thermal conductivity. Moreover, each graphene layer has a number of unusual characteristics, for example its molecular structure is not permeable to very small molecules such as H_2. or noble gas [6], and it shields electromagnetic waves (ultraviolet, visible, infrared and microwaves), etc.

In addition, the mechanical properties are impressive, with a reported Young's modulus of 1TPa [7]. Another important advantage that makes graphite nanoplatelets particularly interesting for structural applications is the relatively simple process required for mass production. Indeed, unlike traditional graphitic nanoreinforcements (CNT and CNF) which require complex and expensive processes, such as chemical vapor deposition and laser vaporization [8, 9], nanoplatelets can be produced from natural graphite through simple techniques [10, 11].

This project is aimed towards the design, manufacturing and characterization of a polymer nanocomposite embedding graphene nanoplatelets (GNP) within a LDPE matrix. LDPE is a cheap, easy-recyclable, engineered thermoplastic that is largely used for packaging applications and it was chosen as the matrix material because of the possibility to also use the resulting composite as a structural material once its mechanical properties are improved.

To analyse the morphology of the composites scanning electron microscopy (SEM), transmission electron microscopy (TEM) and X-ray diffraction (XRD) analysis were conducted in order to determine the dimensions of the nanofiller, and mechanical and thermal properties were evaluated with several tests on nanocomposite films. Samples were obtained using different manufacturing processes in order to analyse the orientation effect of the nanoreinforcements.

2. Material preparation

A composite material based on graphene nanoplatelets embedded into a LDPE matrix was produced by dispersing large aggregates of graphene into the molten polymer using a micro-extruder. Graphene aggregates were obtained by breaking up small pieces of the fragile “graphene sponge” structure, which results from the drying of a concentrated colloidal suspension (ca. 33 g/l) of graphene in acetone. These colloidal graphene suspensions were prepared by exfoliation of expanded graphite using ultrasound. Either a powerful sonication bath or sonication tip can be used, but in order to achieve a complete exfoliation, the expanded graphite must be slowly added to the colloidal suspension during the sonication treatment. The expanded graphite was obtained through the fast heating of mildly oxidized graphite (expandable graphite). Specifically, expandable graphite flakes were placed into a steel crucible covered by a metallic mesh and allowed to expand in air by applying a strong thermal

shock; a muffle furnace set at ca. 800°C was used for the expansion process using a heating time of 4 min. The obtained expanded graphite was dispersed in octane (Aldrich, 98%) by gradually adding it to the liquid phase; intensive sonication was applied to this liquid phase using a tip-sonicator (Hielshier, 1000W) in order to achieve a complete exfoliation of the expanded graphite, resulting in a silvery-grey colloidal suspension. This concentrated (paste) suspension was allowed to air dry at room temperature for 24h in order to obtain the fragile graphite sponge, which was subsequently broken into the small grains required for the nanocomposite preparation.

Samples were obtained using two different manufacturing techniques: compression moulding (*Figure 1a*) and blown extrusion (*Figure 1b*), in order to investigate how the mechanical properties are affected by the orientation of the GNPs within the polymeric matrix.

Because of the irregularity of the nanoplatelets, their orientation inside the LDPE is strongly influenced by the manufacturing process, resulting in a two-dimensional random distribution for the compression moulding (*Figure 1c*) and in a more aligned three-dimensional orientation for the blown extruded samples (*Figure 1d*). As a consequence, samples obtained with blown extrusion will present a higher level of anisotropy in comparison with the samples manufactured by compression moulding.

3. Results and discussion

Figure 2a shows the microstructure of expandable graphite flakes (i.e., graphite intercalated by sulfuric acid molecules) before and after the thermal shock treatment. As can be seen, a worm-like structure is produced at the end of the expansion process because of the gas produced by the following reaction: $C + H_2SO_4 = CO_2 + H_2O +$

SO_2. The solid phase produced at the end of the sonication and drying process consists of GNPs with a thickness of 20 nm and a length of 1 micron (*figure 2b*). `

3.1 XRD Analysis:

In order to analyse the structure of the nanocomposites, XRD was conducted using CuK_α radiation with a wavelength of 1.5406 Å.

The analysis clearly provides some evidences that a significant exfoliation process has taken place during the material processing stage. In fact, the very intensive diffraction peak contained in the diffraction pattern of graphite and generated by the (002) planes (see Figure 3a) is almost completely disappeared in the final composite material. Visibly, the diffractogram shown in Figure 3b contains, in addition to the two main peaks of the LDPE crystallites (which are placed over the diffuse-alone generated by the amorphous fraction of the polymer) at 21.26° and 23.61°, only a low intensity peak at 26.27° corresponding to the (002) planes of graphite nanoplatelets (GNP) present in the sample [10, 12-14] which increases with the percentage of GNPs within the polymer matrix (Figure 3c). A TEM image of thin slices of film cross-section confirm the presence of these graphite nanoplatelets having a thickness of ca. 14nm (see Figure 3d). The obtained XRD diffractogram also proves the presence of an extended iso-orientation of these graphite nanoplatelets in the nanocomposite film, because the (002) peak is the only clearly visible signal of the GNP diffraction pattern which is visible in the nanocomposite diffractogram.

3.2 Thermal Analysis

Mechanical properties of a polymer based composite are strongly dependent on the amount of crystalline phase of the matrix, therefore, since LDPE is a semi-crystalline

material, it is important to establish whether the degree of crystallinity is affected by the presence of graphene nanoplatelets. Therefore, DSC analyses were conducted on pure LDPE, and a comparison was made with composites with increasing filler content. Samples weighting 8 mg were cooled down to 25 °C and then heated up to 120 °C at a rate of 10 °C/min under nitrogen atmosphere to eliminate the thermal history of the sample. *Figure 4* illustrates the thermograms for LDPE and LDPE/GNP composites, showing the same patterns for all the curves, with melting peaks at a temperature of 109-110 °C. The degree of crystallinity for all the samples was calculated using the equation $W_c^{DSC}=\Delta H_f/\Delta H°$, where ΔH_f was estimated by integrating the melting peak for each sample and $\Delta H°$ is the reference heat of fusion (293 $J \cdot g^{-1}$) for polyethylene with 100% crystallinity grade [15].

By analysing the results it is possible to conclude that the inclusion of GNPs within the LDPE matrix does not affect the mass percent of crystallinity of the polymer , therefore the variation of the mechanical properties of the composite cannot be attributed to a microscopic modification of the polymer structure, but is related to the macroscopic reinforcement effect, due to the presence of the nanoscaled filler. Similar results are reported in literature for carbon nanotube/polymer and Graphene/PVA nanocomposites [16, 17].

3.3 Dynamic Mechanical Analysis, Frequency Sweep

The dynamic behaviour of the composite was investigated with DMA tests conducted on LDPE specimens with an increasing amount of GNPs. Samples were tested in tensile mode at room temperature (25 °C) at multiple frequencies, between 10^{-2} and 10^{1} Hz. In order to test all the samples within the viscoelastic range, tests were conducted with a strain of 0.1%.

Data obtained from the test are summarised in *Figure 5* and *6* and they represent the behaviour of storage modulus, loss modulus and tan delta for pure LDPE and LDPE with 3 wt.% and 5 wt.% nanoplatelets concentrations. The data show an increase in the general trend of the storage modulus as the frequency increases and an enhancement of its absolute value with increasing nanoplatelets content (*Figure 5a*). The shift between the curves of LDPE and LDPE3%G is approximately 15%. A similar increment was observed when increasing the nanofiller content from 3 to 5 wt.%. The behaviour of storage modulus can be explained by two different mechanisms. First, the mobility of the polymer chains is restricted by the interaction between the polymer matrix and the GNPs due to their large surface area, resulting in a stiffened interphase. Secondly, increasing the percentage of nanofiller within the polymer, GNPs form a mechanically stable network inside the matrix and the high storage modulus of polymer/GNP contributes to the increase of the modulus of the composite [18].

The behaviour of loss modulus versus frequency is shown in *Figure 5b*, and the general trend seems to be unaffected by the increase in frequency. However, as the amount of nanoreinforcement within the polymer grows, it leads to higher absolute values of loss modulus, which is increased by 16% for a 3wt.% GNP concentration and 14% for a 5 wt.% concentration. Another important parameter in characterising the mechanical properties of a composite is the mechanical damping (*tan delta*), shown in *Figure 5c*. Results show an overall reduction in damping as frequency is increased (which has been reported for LDPE in previous works [19]), and a slight decrease in tan delta passing from LDPE (0.150) to LDPE5%G (0.145) is recorded. Because tan delta is obtained by the ratio of loss modulus (proportional to the energy dissipated during each cycle) to storage modulus (proportional to the total amount of

energy that is stored during each cycle), such behaviour is consistent with the other results obtained and it confirms the increase in brittleness of the GNP based LDPE nanocomposites.

3.4 Mechanical Analysis, Tensile Test:

To investigate the mechanical performance of the LDPE/GNP composites, samples were tested using an Instron 3369 Tensile test Machine. The crosshead speed was set at 100 mm/min in accordance with EN ISO 527-1:1996.

3.4.1 Compression moulding samples

Figure 7a shows some representative stress-strain curves for LDPE and LDPE/GNP composites, manufactured using the compression moulding technique with an increasing percentage of nanoreinforcement (3 wt.% and 5 wt.%). The inlets in the stress-strain figures show the variation of the slopes for all the samples. As a consequence of the pressure applied, GNPs are orientated randomly in plane, leading to an in-plane isotropy. It can be seen that LDPE with a GNP loading of 3 wt.% shows a 15% increase in Young's modulus going from 301 MPa of the pure LDPE to 347 MPa. Increasing the GNP content to 5 wt.%, the elastic modulus is increased by an additional 16%, reaching 407 MPa. However, as the nanofiller content is increased, maximum strain dramatically decreases from 5.8 to 0.33, while a slight decrease in maximum stress (from 16 MPa to 12 MPa) was also observed. The presence of the GNPs within the LDPE matrix strongly affects the ductility of the polymer, shifting the stress strain curves to a more brittle behaviour. As shown in *Figure 7b*, while after yielding LDPE is capable of withstands much greater extension (up to 600%) by activating necking and cold-drawing mechanisms, GNP based composites exhibit a

very small plastic region (covering strains of 20-30%) resulting in an almost brittle fracture immediately after the yield point (*Figure 7c*). The reason for this modification may be attributed to the reduced polymer mobility due to the presence of graphene sheets. Indeed, the large aspect ratio of the filler and the interaction with the LDPE matrix can obstruct the reciprocal chains' movements, resulting in a more brittle material [20]. Moreover, the reduction in tensile strength could be explained by the presence of relatively large inhomogeneities (graphite agglomerates) within the LDPE matrix that lead to structural imperfections and that can generate premature cracks [21, 22].

3.4.2 Blown extrusion samples

As explained in section 2, blown extrusion process leads to composites films characterised by a high grade of anisotropy. Because the material is stretched after the insufflations of air, GNPs will be orientated in the direction of the flow, resulting in a material which is characterised by different mechanical properties in the machine direction (MD) and in transverse direction (TD). The first series of tests were carried out on unreinforced LDPE, and are shown in *figure 8a*. As it is possible to observe from the differences in the stress-strain curves, LDPE shows a behaviour which is very similar to the one observed for compression moulded samples in transverse direction (TD), however the maximum strain reached is only 300%, while it was almost twice this value for the unreinforced LDPE. The orientation effect of the polymeric chains is clearly shown in the curve relative to the machine direction (MD) samples where LDPE acts more like a brittle material, reaching higher values of tensile strength but a lower maximum strain. Similar results were reported by Guichon [23]. Another important consideration regarding the Young's modulus value

is that the properties are only slightly changed in the transverse and machine directions (180 MPa for TD and 185 MPa for MD), meaning that the orientation of the chains affects principally the necking and re-crystallisation phases and not the elasticity of the polymer. In *figure 8b* the stress-strain curves for nanoreinforced LDPE with 5 wt.% of GNPs in both machine and transverse direction is shown. As for pure LDPE, it is possible to observe the effect produced by the orientation of the graphene nanoplatelets. In the transverse direction a brittleness similar to that of a compression moulded nanocomposite is observed, while in the machine direction the orientation of GNPs leads to higher tensile strength (increasing from 15 to 23 MPa) and also higher strain (increasing from 0.7 to 1.1). Young's modulus dependence on the orientation is more pronounced in the case of the composite than for the neat polymer, increasing from 430 to 477MPa. This behaviour can be explained because the presence of oriented GNPs affects the elastic behaviour of the composite, increasing its stiffness. *Figure 9a* and *9b* illustrates the stress-strain curves comparison for neat LDPE and GNP composites for blown extruded film in transverse and machine directions. The Young's modulus is increased for both TD (from 180 to 425 MPa) and MD (from 187 to 477 MPa) (*see figure 10*), while the maximum strain is reduced by 75% for TD and by 10% for MD. However, regarding maximum stress, for TD samples the doping of GNPs within the LDPE matrix leads to an increase of tensile strength of 30%, while for MD samples it was almost constant (a small reduction is recorded, which falls within the bounds of intrinsic experimental error).

3.4.3 Halpin-Tsai Young's modulus evaluation model

The Halpin-Tsai model is widely used to predict the elastic modulus of both unidirectional and randomly distributed nanofiller-reinforced polymers [17, 24, 25].

Considering the compression moulded LDPE/GNP samples, the Halpin-Tsai equation is written as:

$$E_{random} = E_p \left[\frac{3}{8} \frac{1+\left(\frac{2l_G}{3t_G}\right)\eta_L V_G}{1-(\eta_L V_G)} + \frac{5}{8} \frac{1+(2\eta_T V_G)}{1-(\eta_T V_G)} \right] \quad (1)$$

$$\eta_L = \frac{\left(\frac{E_G}{E_P}\right)-1}{\left(\frac{E_G}{E_P}\right)+\left(\frac{2l_G}{3t_G}\right)} \quad (2)$$

$$\eta_T = \frac{\left(\frac{E_G}{E_P}\right)-1}{\left(\frac{E_G}{E_P}\right)+2} \quad (3)$$

Where E is the Young's Modulus of the composite with randomly oriented nanofillers, E_p and E_g are the tensile moduli of LDPE (obtained from the tensile test) and graphene (~1 TPa), l_G, t_G and V_G are respectively the length of one GNP (~1 μm), its thickness (~20 nm) and the volume fraction of the nanoreinforcement, which is calculated from the weight fraction.

The results in *figure 11a* illustrate how the experimental data match the theoretical model. For blown extruded samples, GNPs are oriented in the flow direction, therefore the Halpin-Tsai equation becomes:

$$E_{oriented} = E_p \left[\frac{1+\left(\frac{2l_G}{3t_G}\right)\eta_L V_G}{1-(\eta_L V_G)} \right] \quad (4)$$

Figure 11b shows the comparison between the theoretical model and the experimental data for the blown extruded LDPE/GNP composites. As it can be seen from the curves, the experimental value of Young's modulus for the composites is higher than that predicted by the Halpin-Tsai equation by almost 50%. One possible explanation for this difference could be due to the dimensions of the nanoplatelets after the manufacturing process. During the extrusion process, GNP are strongly stretched in the machine direction, therefore, because the different graphene layers are bonded

together only by weak van der Waals forces, this stretching effect could lead to a thinning of the graphene nanoplatelets. This thickness reduction is confirmed by the matching of the experimental data with the 10 nm thickness theoretical curve.

4. Conclusion

Graphene nanoplatelets reinforced LDPE composites were prepared by incorporating dried nanoplatelets obtained by exfoliation of expanded graphite within a low-density polyethylene matrix. The thickness of GNP was evaluated by SEM analysis, and an average value of 20 nm and length of ~ 1 μm was found. XRD analysis was carried out to evaluate the presence of GNPs within the composites and the results confirm the semi-crystalline structure of LDPE with the detected peak at ~26.5° related to the distance between the different layers of graphene nanoplatelets. The amplitude of this peak increases with the percentage of GNPs within the polymeric matrix. Thermograms obtained by DSC analysis were analysed in order to fully understand the effect of GNPs on the microscopic structure of the LDPE and the results show that the inclusion of the nanofillers does not affect the mass percent crystallinity of the polymer. As a consequence, the variation of the mechanical properties of the nanocomposite cannot be attributed to a microscopic modification of the polymer structure, but only to the macroscopic reinforcement effect caused by the presence of the nanoscaled filler. DMA data show an increase in both storage and loss modulus. For compression moulded samples, an increase of the tensile modulus of ~30% for a 3 wt.% GNP and of 36% for a 5 wt.% of GNP is reported. Moreover, the stress-strain curve of the composites exhibits a very small plastic region resulting in an almost brittle fracture in comparison with the pure LDPE, due to the presence of large graphite agglomerates. Blown extruded samples exhibited a high level of anisotropy due to the stretching of LDPE and GNPs during the manufacturing process. For both

machine and transverse direction samples the presence of GNPs leads to a larger increase in the tensile modulus (~135% in transverse direction and ~160% in machine direction) resulting in more brittle behaviour for the TD samples. Tensile strength is increased by almost 30% in transverse direction, while it stays constant for the machine direction samples. This effect can be attributed to the LDPE's ability to activate necking and cold-drawing mechanisms resulting in recrystallisation. Results obtained by tensile tests were compared with the Halpin-Tsai model showing good matches for samples obtained with compression moulding (in-plane randomly oriented nanofillers), while the experimental data curve for blown extruded samples (highly oriented nanoplatelets) presented slightly higher values than the theoretical model. This result can be explained by a reduction in the thickness of GNPs within the polymeric matrix due to the strong orientation acquired during the extrusion process.

Acknowledges

Authors Authors would like to acknowledge Dr Simon Pickering and Diego Colombara from the University of Bath for the many valuable suggestions during this work.

References:

[1] Chisholm N, Mahfuz H, Rangari VK, Ashfaq A, Jeelani S. Fabrication and mechanical characterization of carbon/SiC-epoxy nanocomposites. Composite Structures. 2005;67(1):115-24.

[2] Lange FF, Radford KC. Fracture energy of an epoxy composite system. Journal of Materials Science. 1971;6(9):1197-203.

[3] Faber KT, Evans AG. Crack deflection processes—I. Theory. Acta Metallurgica. 1983;31(4):565-76.
[4] Johnsen BB, Kinloch AJ, Mohammed RD, Taylor AC, Sprenger S. Toughening mechanisms of nanoparticle-modified epoxy polymers. Polymer. 2007;48(2):530-41.
[5] Stankovich S, Dikin DA, Piner RD, Kohlhaas KA, Kleinhammes A, Jia Y, et al. Synthesis of graphene-based nanosheets via chemical reduction of exfoliated graphite oxide. Carbon. 2007;45(7):1558-65.
[6] Bunch JS, Verbridge SS, Alden JS, van der Zande AM, Parpia JM, Craighead HG, et al. Impermeable Atomic Membranes from Graphene Sheets. Nano Letters. 2008;8(8):2458-62.
[7] Jiang J-W, Wang J-S, Li B. Young's modulus of graphene: A molecular dynamics study. Physical Review B. 2009;80(11):113405.
[8] Guo T, Nikolaev P, Thess A, Colbert DT, Smalley RE. Catalytic growth of single-walled manotubes by laser vaporization. Chemical Physics Letters. 1995;243(1-2):49-54.
[9] Breuer O, Sundararaj U. Big returns from small fibers: A review of polymer/carbon nanotube composites. Polymer Composites. 2004;25(6):630-45.
[10] Fim FdC, Guterres JM, Basso NRS, Galland GB. Polyethylene/graphite nanocomposites obtained by in situ polymerization. Journal of Polymer Science Part A: Polymer Chemistry. 2010;48(3):692-8.
[11] Kumar S, Sun LL, Caceres S, Li B, Wood W, Perugini A, et al. Dynamic synergy of graphitic nanoplatelets and multi-walled carbon nanotubes in polyetherimide nanocomposites. Nanotechnology. 2010;21(10):105702.
[12] Lian P, Zhu X, Liang S, Li Z, Yang W, Wang H. Large reversible capacity of high quality graphene sheets as an anode material for lithium-ion batteries. Electrochimica Acta. 2010;55(12):3909-14.
[13] Yang J, Zhang L-Q, Shi J-H, Quan Y-N, Wang L-L, Tian M. Mechanical and functional properties of composites based on graphite and carboxylated acrylonitrile butadiene rubber. Journal of Applied Polymer Science. 2010;116(5):2706-13.
[14] Jacob George J, Bandyopadhyay A, Bhowmick AK. New generation layered nanocomposites derived from ethylene-co-vinyl acetate and naturally occurring graphite. Journal of Applied Polymer Science. 2008;108(3):1603-16.

[15] Morawiec J, Pawlak A, Slouf M, Galeski A, Piorkowska E, Krasnikowa N. Preparation and properties of compatibilized LDPE/organo-modified montmorillonite nanocomposites. European Polymer Journal. 2005;41(5):1115-22.

[16] Liu L, Barber AH, Nuriel S, Wagner HD. Mechanical Properties of Functionalized Single-Walled Carbon-Nanotube/Poly(vinyl alcohol) Nanocomposites. Advanced Functional Materials. 2005;15(6):975-80.

[17] Liang J, Huang Y, Zhang L, Wang Y, Ma Y, Guo T, et al. Molecular-Level Dispersion of Graphene into Poly(vinyl alcohol) and Effective Reinforcement of their Nanocomposites. Advanced Functional Materials. 2009;19(14):2297-302.

[18] RamanathanT, Abdala AA, StankovichS, Dikin DA, Herrera Alonso M, Piner RD, et al. Functionalized graphene sheets for polymer nanocomposites. Nat Nano. 2008;3(6):327-31.

[19] Documentation PE. Characterization of LDPE Over a Large Frequency Range. 2007 [cited; Available from: http://www.perkinelmer.com/CMSResources/Images/44-74196APP_LDPECharacterization.pdf

[20] Kuilla T, Bhadra S, Yao D, Kim NH, Bose S, Lee JH. Recent advances in graphene based polymer composites. Progress in Polymer Science. 2010;35(11):1350-75.

[21] Zheng W, Lu X, Wong S-C. Electrical and mechanical properties of expanded graphite-reinforced high-density polyethylene. Journal of Applied Polymer Science. 2004;91(5):2781-8.

[22] Andrews R, Jacques D, Minot M, Rantell T. Fabrication of Carbon Multiwall Nanotube/Polymer Composites by Shear Mixing. Macromolecular Materials and Engineering. 2002;287(6):395-403.

[23] Guichon O, Séguéla R, David L, Vigier G. Influence of the molecular architecture of low-density polyethylene on the texture and mechanical properties of blown films. Journal of Polymer Science Part B: Polymer Physics. 2003;41(4):327-40.

[24] Zhou T, Chen F, Tang C, Bai H, Zhang Q, Deng H, et al. The preparation of high performance and conductive poly (vinyl alcohol)/graphene nanocomposite via reducing graphite oxide with sodium hydrosulfite. Composites Science and Technology. 2011;71(9):1266-70.

[25] Zhao X, Zhang Q, Chen D, Lu P. Enhanced Mechanical Properties of Graphene-Based Poly(vinyl alcohol) Composites. Macromolecules. 2010;43(5):2357-63.

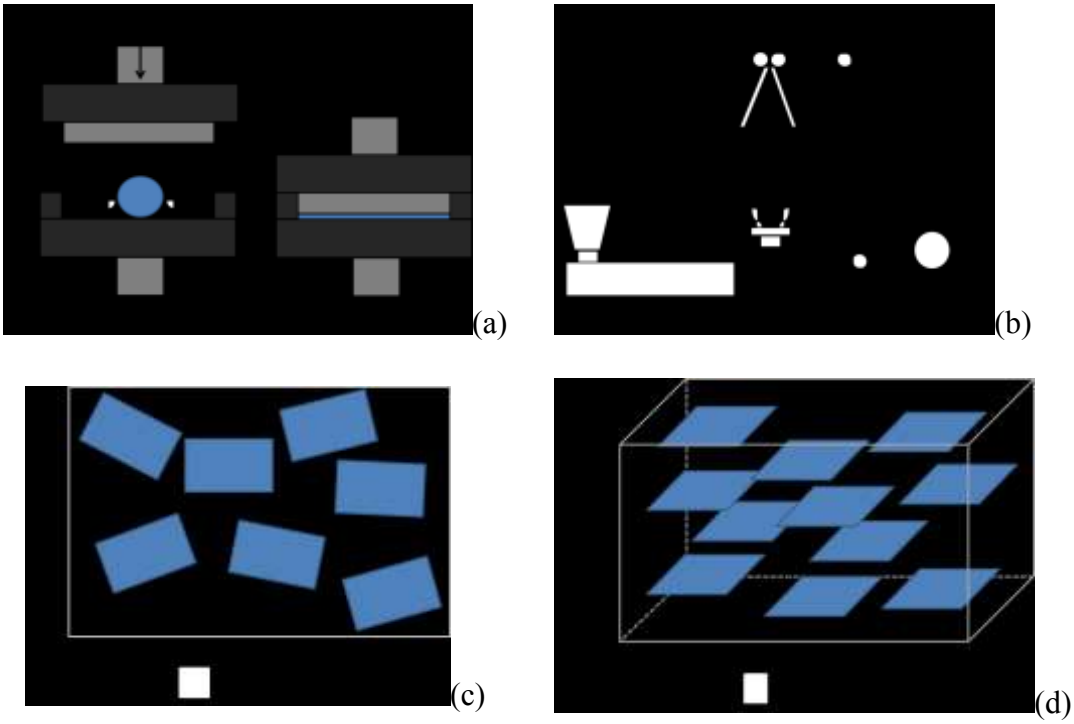

Figure 1 – a) Schematic of Compression Moulding process; b) Schematic of Blown Extrusion process; c) Schematics of randomly in plane oriented nanoparticles; d) Schematics of three-dimensional nanoparticles

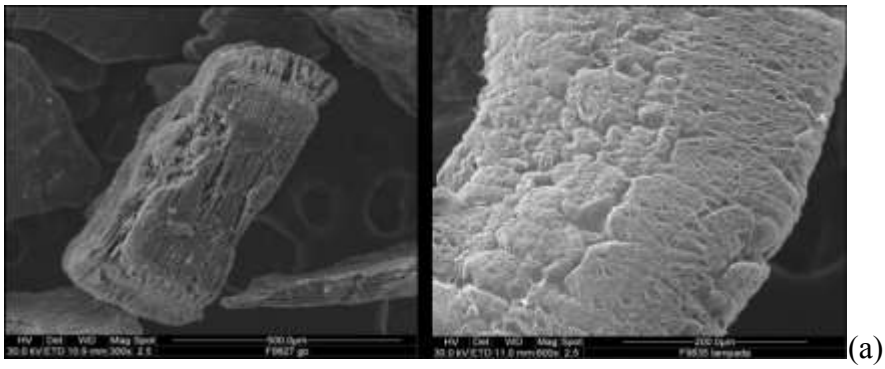

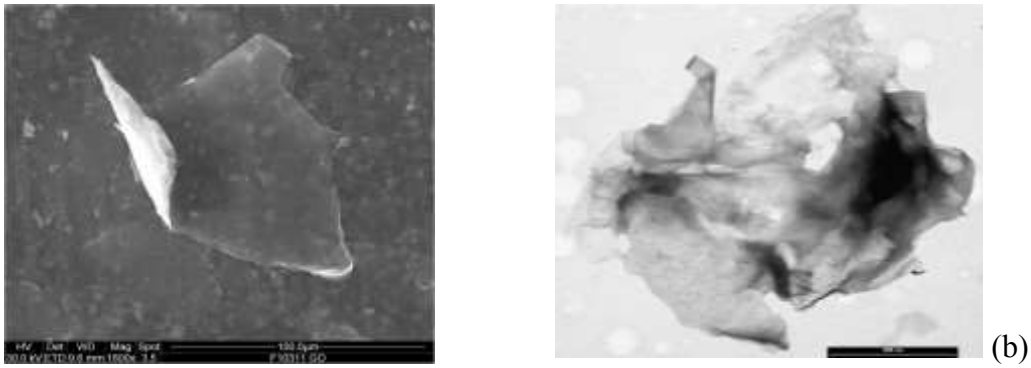

Fig. 2 – a) SEM micrograph of the expandable graphite flake (left side) and of expanded graphite filament (right side) ; b) SEM micrographs of GNP after the drying process

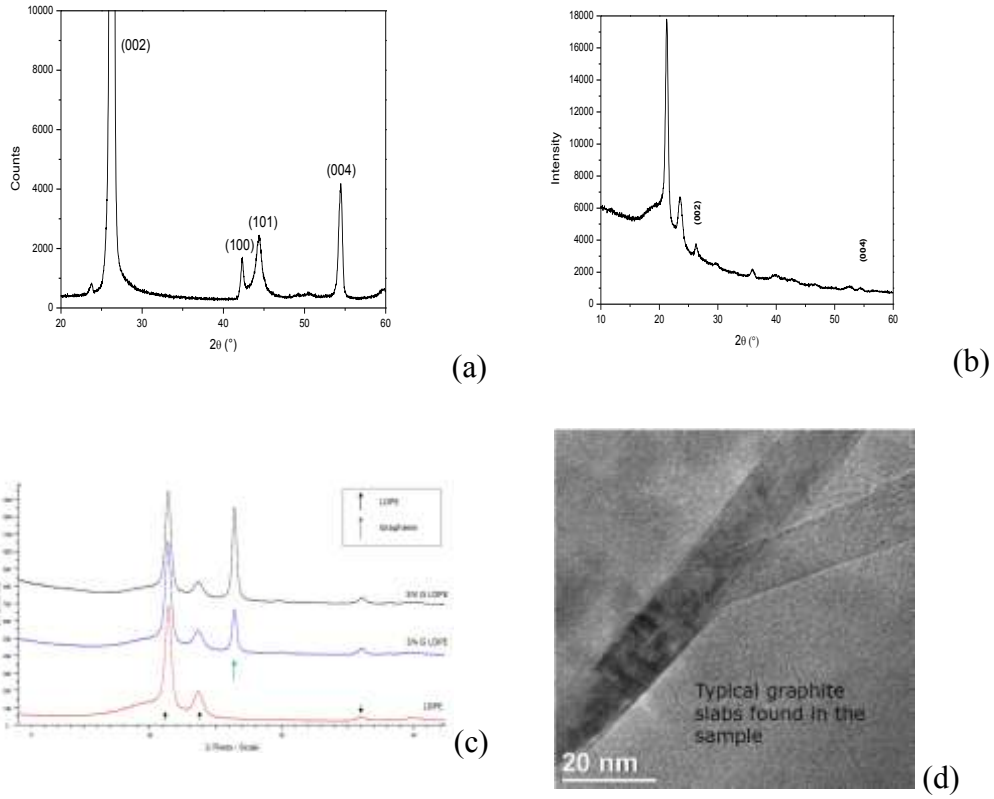

Figure 3 - XRD of graphite (a), LDPE/GNP composites (b) and effect of GNP concentration (c). Figure (d) represents the typical microstructure of the LDPE/GNP composite

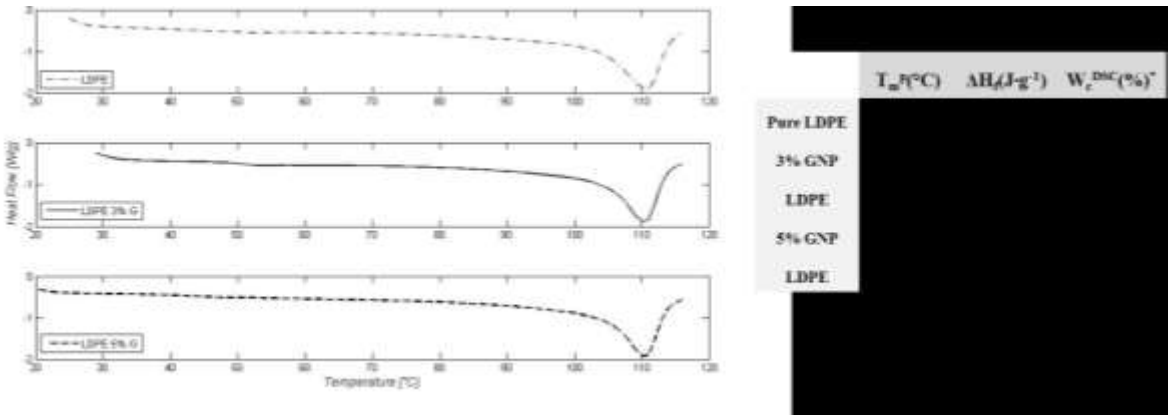

Figure 4 - DSC thermograms and results for LDPE and LDPE/GNP nanocomposites

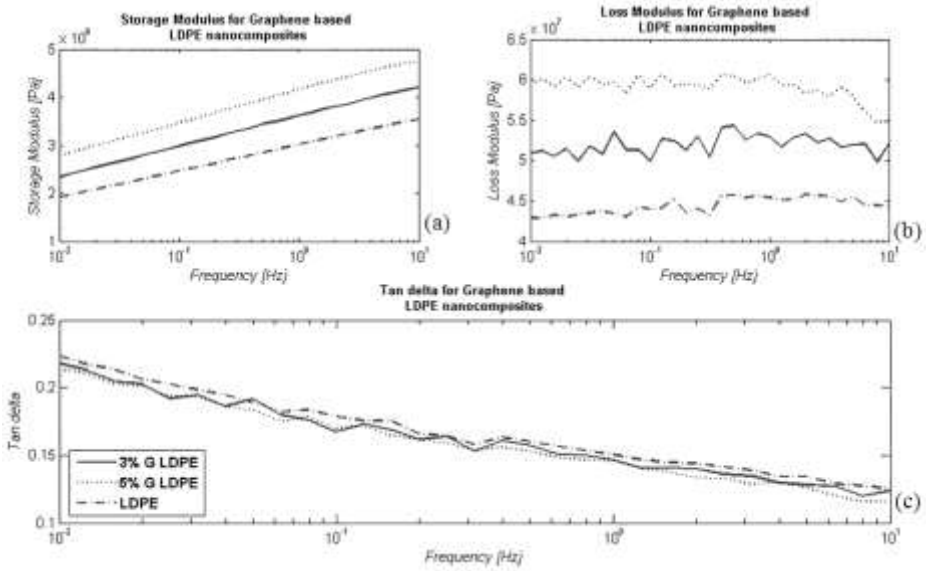

Figure 5 – DMA frequency sweep curves for LDPE/GNP composites: (a) storage modulus, (b) loss modulus, (c) Tan delta

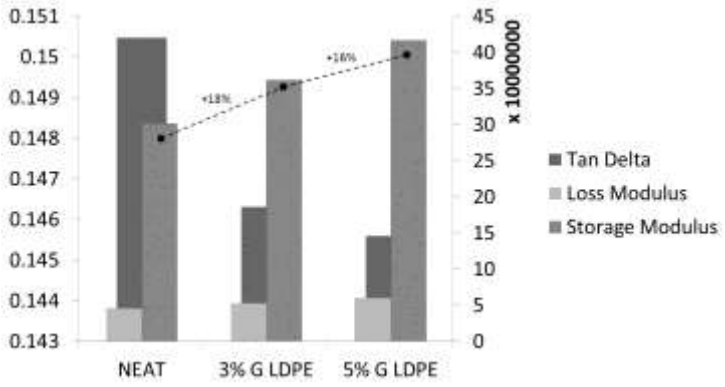

Figure 6 - Storage Modulus, Loss Modulus and Tan delta results at 1Hz for LDPE and LDPE/GNP composites

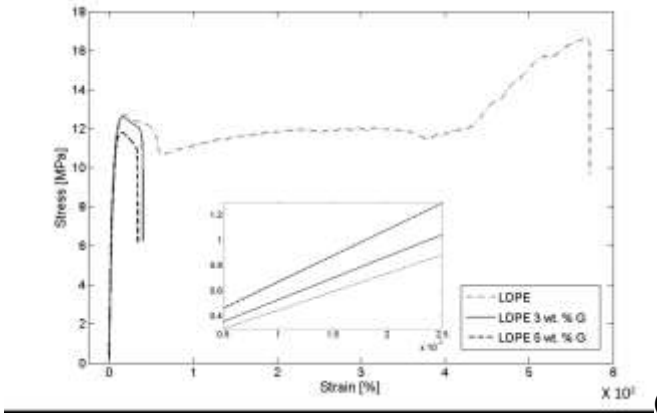

(a)

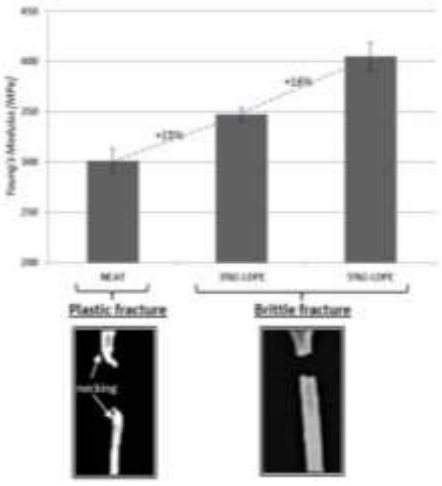

(b)

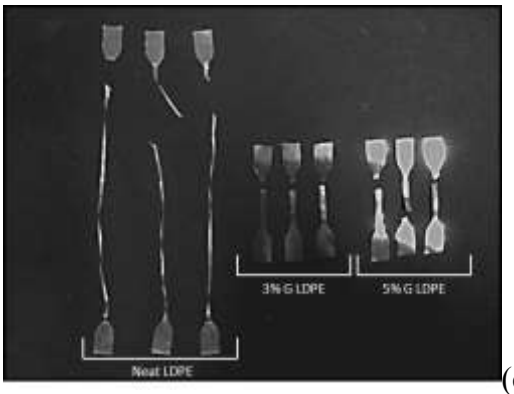

(c)

Figure 7 – a) Stress-Strain curves for neat LDPE and composites with increasing content of GNP. The inlet shows the slopes of the curves**; b)** Relation between Young's modulus increasing and change in fracture mode for LDPE and LDPE/GNP composites; c) LDPE and LDPE/GNP composite samples after tensile test

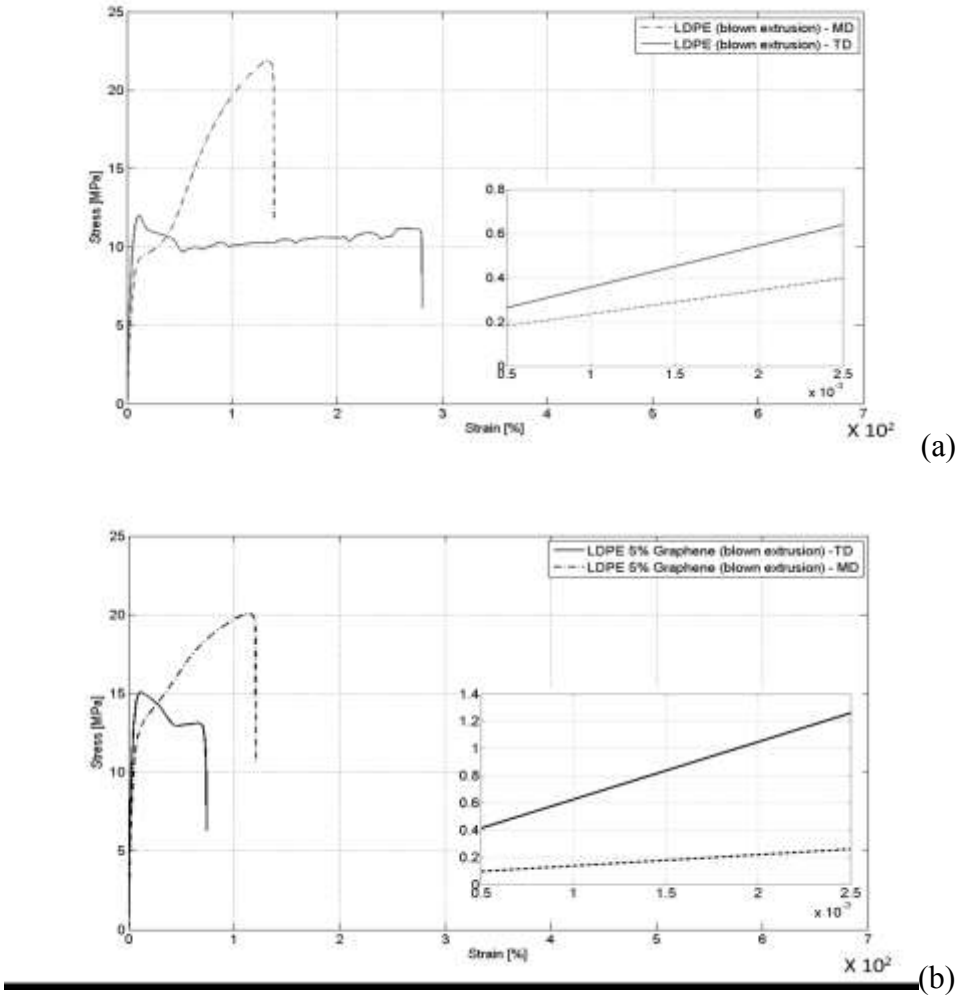

Figure 8 – a) Stress-Strain curves for neat LDPE in blown extrusion process; b) Stress-Strain curves for LDPE/GNP composites in blown extrusion process. **The inlets show the slopes of the curves.**

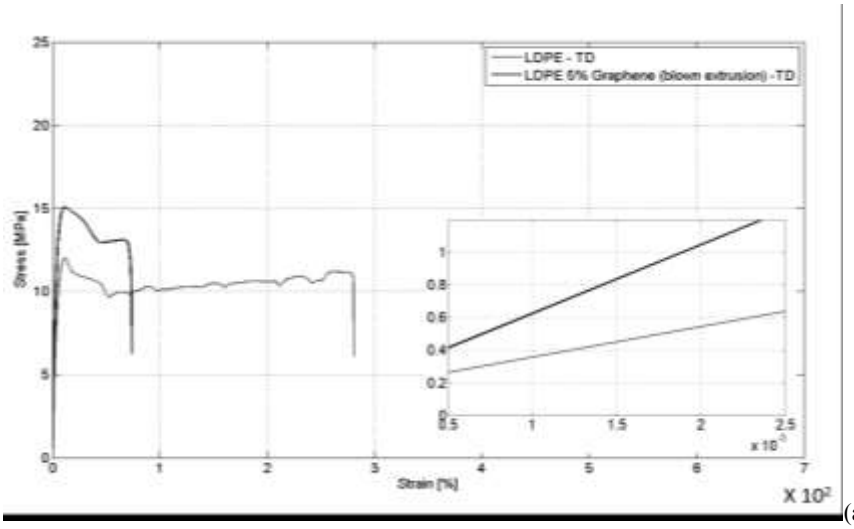

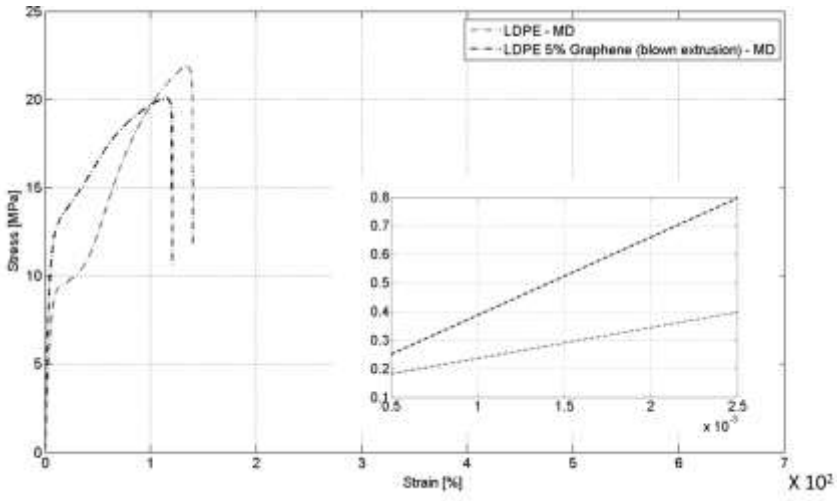

(b)

Figure 9 – Comparison between Stress-Strain curves for LDPE/GNP composites and pure LDPE in transverse direction (a) and machine direction (b); **The inlets show the slopes of the curves.**

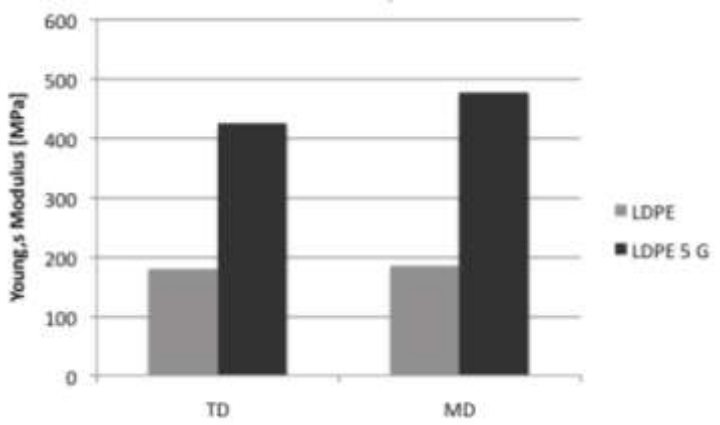

Figure 10 - Young's modulus increase for LDPE/GNP in both transverse and machine direction.

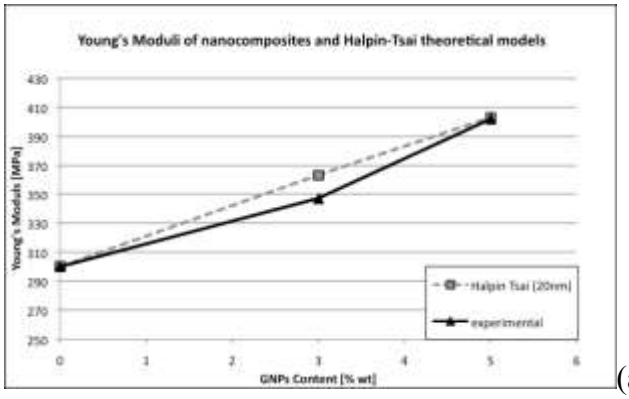

(a)

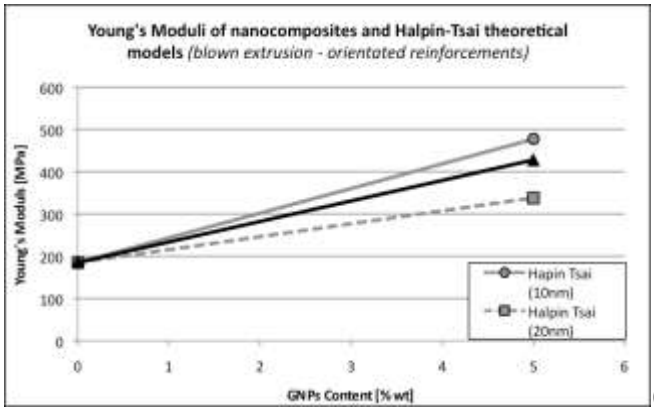

(b)

Figure 11 – a) Comparison between Halpin-Tsai modulus evaluation model and experimental data for compression moulded LDPE/GNP composites; **b)** Comparison between Halpin-Tsai modulus evaluation model and experimental data for blown extruded LDPE/GNP composites